Adam ŚWITOŃSKI[1,3], Tomasz BŁACHOWICZ[2], Marcin ZIELIŃSKI[4], Marta MISIUK-HOJTO[4], Konrad WOJCIECHOWSKI[1,3]

Polsko Japońska Wyższa Szkoła Technik Komputerowych, Wydział Zamiejscowy Informatyki w Bytomiu (1),
Politechnika Śląska, Instytut Fizyki (2), Politechnika Śląska, Instytut Informatyki (3),
Akademia Medyczna we Wrocławiu, Katedra i Klinika Okulistyki (4)

Ophthalmic diagnosis based on multispectral imaging

Abstract. *We have proposed and deployed prototyped multispectral capturing device for the ophthalmic diagnosis. The main component of the device are slit lamp, liquid crystal tunable filter and high sensitive monochrome camera. The applied hardware allows to obtain 21 spectral channels in the visible light range. The device has been calibrated based on the captured images of the colorchecker colors with known RGB and spectral values.. The proposed device is focused on the diagnoses of cancer, PEX, galucoma and diabetic retinopathy,.*

Steszczenie*. W ramach pracy zaproponowano urządzenie obrazowania wielospektralnego na potrzeby diagnostyki okulistycznej. Główne komponenty urządzenia to lampa szczelinowa, elektrycznie przełączalny filtr ciekłokrystaliczny oraz wysokiej czułości kamera monochromatyczna. Wybrane rozwiązania sprzętowe.. pozwalają na uzyskanie 21 kanałów spektralnym w zakresie światła widzialnego. Urządzenie zostało skalibrowane na podstawie zdjęć próbnika kolorów. Przewiduje się zastosowania opracowanego urządzenia w diagnostyce zmian nowotworowych, zespołu PEX, jaskry i retinopatii cukrzycowej. (**Diagnostyka okulistyczna na bazie wielospektralnego obrazowania gałki ocznej**)*.

Keywords: mutlispectral imaging, ophthalmic diagnosis, retina, anatomical structures of the eye
Słowa kluczowe: obrazowanie wielospektralne, diagnostyka okulistyczna, dno oka, struktury gałki ocznej

Multispectral imaging

Multispectral image contains spectral data of its every pixel and is represented by the function $I(x,y,\lambda)$. It has the structure of three dimensional image cube, where two dimensions are responsible for spatial and the third one is of the spectral domain. In fact, the image gives information of the intensities I of the radiance with the specified wavelengths λ which are measured in different image points (x,y). The accuracy of the spectrum estimation depends on the number of image channels - wavelengths in which intensity is captured. A multispectral image contains much more information than a typical color image. It gives detailed spectrum data of its every pixel, in contrast to the color image, which has only some kind of aggregation of the spectrum.

There are numerous areas in which multispectral imaging is applied - Biomedicine: There are lots of diseases and pathological areas which are noticeable in the spectral space. Tumor and cancer detection are best examples [3],[4],[5],[16],[17],[18]. Geography and geology: Collecting spectral data by the land information systems help to improve more detailed objects detection and classification, for instance rocks, soils and vegetation. Example method could be found in [19] ; Agriculture and forestry: It makes easier to evaluate the state of plants population, ocean flora or forest stands and allows for a deeper analysis. [20] applied hyperspectral imagery for the detection of vegetation of ten different classes ; Archeology and art history: It is used in verifying the authenticity of works of arts, as for instance paintings or books and detecting some hidden contents.[21] analyze 16th century paintings to characterize the paint layers within micro samples based on the multispectral imaging. and many others like biology, crime detection, salvage service, meteorology, etc.

Selected ophthalmic diagnoses

The multispectral imaging can be applied in any diagnosis of eye structures. However the idea of constructing the prototype multispectral capturing device was based on the our earlier experiences and analysis of the methods proposed in the literature for diagnoses of cancer, PEX disease, glaucoma and diabetic retinopathy.

The cancerous changes of sight organs can be placed on any of the eye structures: eyelids, cornea, iris, sclera, anterior and posterior chambers of the eye and retina. The preliminary diagnosis is usually performed on the basis of visual inspection of the eye structures by the medical expert. However, the discovered, suspicious regions have to be examined in the following tests, usually based on computer tomography, magnetic resonance or histopathology. The direct or even computer supported visual analysis of the colors cannot unambiguously point cancerous tissues .It is because their similarity to other abnormalities, as for instance inflammations. There is much easier discrimination of the cancerous changes in spectral space in comparing to the color space. There are multiple applications of the multispectral imaging for the cancer detection. In [3] the method for the diagnosis of skin tissue is presented. It is based on the spectral signatures of the multispectral image points and supervised machine learning. The method has obtained 99% accuracy for the collected test dataset. Similar method, but focused on support vector machine classifier is presented in [4]. In [5] simulation of fluorescence phenomenon is performed for cancer detection.

PEX disease, pseudoexfoliation syndrome, is a common, age-related fibrillopathy of unknown cause. It is characterized by the deposition of a distinctive fibrillar material in the anterior segment of the eye [6]. PEX is currently considered to be one of the main causes of secondary glaucoma [7]. PEX can be recognized in the advanced stage of the disease, by white-gray deposits forming the typical patterns on the anterior eye structures. The multispectral analysis could improve PEX diagnosis, allowing to detect the disease in its early stages.

There are many abnormalities appearing on the retina. The two most often causes of blindness in the current population are diabetic retinopathy and glaucoma. Thus effective diagnosis of the diseases is a challenging task with crucial social significance. Glaucoma is a disease with degeneration of optic nerve transmitting sight effects from the optic sensors located on the retina to a brain. The partial optic nerve damages, usually caused by the increased pressure, results in the losses in the visible area which can be reconstructed by the perimeter examination [29]. The increased pressure causes the eyecup degeneration, especially in comparing to the shape of the optic disc [30] In [8] the method which uses shape coefficients of the segmented eyecup and optic disc, genetic feature selection technique and multilayer

perceptron classifier is proposed for glaucoma diagnosis. In such approaches, the results are limited to the accuracy of the crucial retinal image segmentation. Numerous methods were proposed for automatic retina segmentation, They are based on watershed transformation [8], Hough transform [9],[10], active contours [11], mathematical morphology [12], template matching [13],[14] or adaptive thresholding [15]. However all of them suffer weak contrast between retina anatomical structures in color spaces. The multispectral imaging should improve the segmentation and in consequence the glaucoma diagnosis.

Diabetic retinopathy is caused by complications of the diabetes which result in retina degenerations. In the first stage of the disease the structure of capillaries is damaged. The locally dilations occur, visible as a small red spots on retina images. Further, the artery strokes appear, The accumulations of lipids and protein causes another lesions called exudates. They are represented by bright, reflective, white or cream colored areas of different sizes on retina, similar to optic disc and eyecup, but with irregular shapes. In the last stage of diabetic retinopathy structure of vascular network is degenerated, forming shapes with greater curvature. There are numerous methods proposed for detecting diabetic retinopathy symptoms based on the color retina images. The microaneurysm can be located by HitMiss operator and watershed transformation [22], blood vessels by top-hat operator applied to the contrast enhanced image [23] or top-hat followed by toggle mapping technique [12] and exudates by geodesic reconstruction [24]. Once again, there is no strict distinction in color spaces of detected abnormalities and anatomical structures. To improve contrast of the blood vessels, microaneurysm and strokes we can use fluorescein angiographies instead fundus eye images [25], but this is a separate, dedicated examination which requires to administer special medicine. Thus, the application of multispectral imaging seems to be reasonable for the diabetic retinopathy diagnosis.

Multispectral capturing device for the ophthalmic diagnosis

On the basis of our earlier experiences in constructing the multispectral capturing device for endoscopic diagnosis [31], we have proposed similar device, but dedicated to ophthalmic diagnosis. Its main component is a liquid crystal tunable filter [2], which is able to control spectral transmission electronically by keeping the band of a selected wavelength and removing the rest. It is possible by the proper polarization of crystal plates. The filter is the front part of the device mounted directly after the optical focusing system. The electromagnetic radiance which passed through the filter is registered by a high sensitivity monochrome camera. The monochrome camera summarizes the radiance from the visible light range. Thus if radiance passes through the filter, the camera registers only the radiance of the specified wavelength. The camera and the filter are synchronized by the described below, dedicated software. Such a process of the multispectral channel acquisition is iterated for all selected wavelengths of the multispectral image. The resolution of the spectral domain depends on the ability of the filter - size of the filtered window. The structure of proposed capturing device is presented in Fig. 1.

The model of the dedicated control software is shown in Fig. 2. The main component is the Main Control Module, responsible for the synchronizing the camera and the filter, iterating channels acquisition and generating events with information of the acquisition progress. The GUI Module and Database Module register proper listeners of the events and they display captured image for the user and store it in the database respectively. The main module communicates with the filter and the camera by the proposed driver interfaces.

To capture retinal images the special Volk lens have to be mounted prior to slit lamp. It make possible to focus radiance passing optical system of an eye..

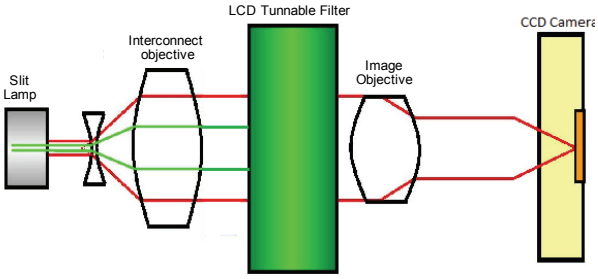

Fig. 1 Structure of the proposed multispectral capturing device

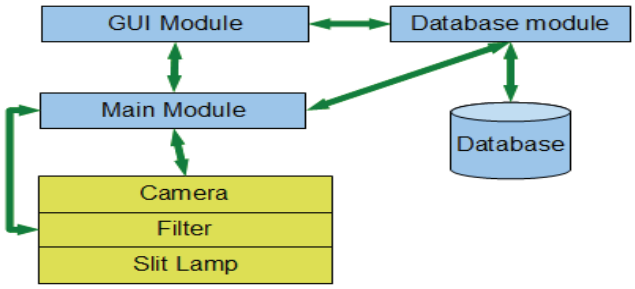

Fig. 2 Control software of the proposed multispectral device

In constructing the device, we have chosen a Varispec liquid crystal tunable filter [28] and an Andor Luca monochrome camera [29]. The above mentioned window size of the filter gets 21 different disjoint spectral channels from the range of the visible light. The average switch time for the filter is about 50ms.

The Andor camera has a low noise CCD matrix, a VGA resolution and a 16 bit grayscale. The acquisition time depends on the intensity of delivered light to the observed objects. It usually requires 40-100ms to take photos at the acceptable level of noise. II is the result of the applied monochrome camera, which summarizes the intensity of the radiances of the whole visible light range. If the radiance passes through the filter which removes the radiance outside specified narrow range, the total intensity is very low, thus it requires a greater acquisition time. To reduce the time we can use more sets of filter-camera and capture different channels asynchronously. During the whole acquisition the objects should be static to achieve the channels with directly corresponding scenes. If they are non-static the special correction techniques have to be applied, for instance, to find transformations between channels and match them we can try to use the optical flow methods.

Prototype model of our multispectral capturing device is presented in Fig. 3 [1]. Example, captured multispectral image with a front part of an eye is presented in Fig. 4.

Calibration of the multispectral device

The spectral dimension of the proposed device is given in the scale of the device not in standardized units. The scale depends on characteristic of the filter – the intensities passing in the following windows and the aggregation abilities of the monochrome camera. The intensities passing by the Varisepc filter is non uniform. The high frequencies – short wavelengths represented blue colors, are smothered

much more in comparing to low frequencies [31], [27]. It causes that following spectral channels of multispectral image are given in the different, directly incomparable scales. The effect of not uniform passing by the filter can be noticed in Fig. 4 – high frequencies are smothered more which results in much greater noise. To reduce the noise , acquisition time has to be increased. What is more, spectral acquisition also depends on the light source – intensity and its spectral properties and acquisition time of the camera. To be able to compare spectra of different scales directly, we have to calibrate the device to the new scale. If we do not know direct properties of the hardware applied we can try to find such a transformation on the basis of trainset – set containing multispectral images with known spectral values in the new scale. The supervised learning techniques can be used [28].

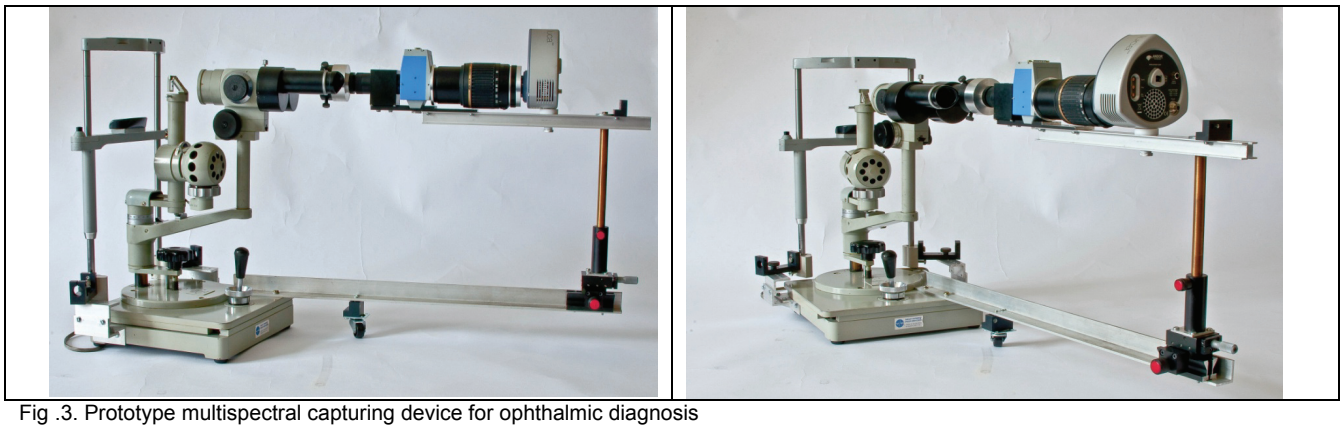

Fig .3. Prototype multispectral capturing device for ophthalmic diagnosis

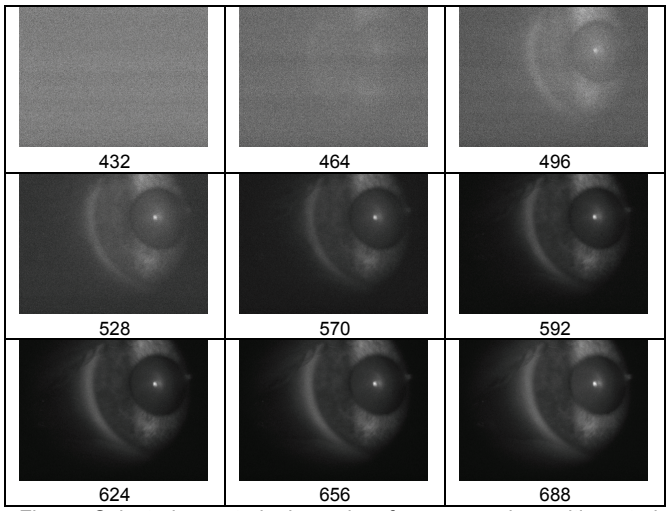

Fig. 4 Selected spectral channels of an example multispectral image represented front part of an eye.

In calibration we have used XRite ColorChecker Classic [32] with given RGB values and spectral values acquired by external much more accurate Ocean Optics spectrometer [33]. We have captured each of the 24 colors and extracted spectral signatures of their middle areas.

We have decided to calibrate the device to RGB color space and to the spectral space of the Ocean Optics. RGB calibration is useful in reconstruction of the original color image for the visualization and quick preview purposes. Calibration to Ocean Optics space makes the following spectral channels to be given in the similar scales. It should improve further numerical processing of the multispectral image supporting medical diagnosis.

We have assumed linear transformation to be sufficient for calibration We have used standard Least Mean Square Regression, Simple Linear Regression and Least Median Square Regression [28]. Simple Linear Regression builds a linear regression model based on the single attribute with the smallest squared error. The Least Median Square Regression iterates the standard linear regression for the subsamples and chooses the one with minimal median squared error. For the spectrum calibration, we have tested two approaches called 1vs1 and ALLvs1. In the 1vs1 spectrum value in the pattern space relies only on the corresponding single value of the multispectral image space. To the contrary, in the ALLvs1 approach it is the linear combination of all the values.

Because of limited paper size, only the RGB calibration results are presented in detail. To evaluate the examined regressors we have split the dataset into train and test parts by cross validation method. In Fig. 5 the mean absolute errors of RGB colors regression are shown. They are below 10% of the global 8bit scale, which seems to be satisfactory.. The longer wavelengths contain less noise, because of the Varispec filter characteristics, which is the reason of more accurate red and green colors regression. The best results have obtained Least Median Square Regressor. Simple Linear and classical Least Mean Square are very similar, still acceptable, but noticeable worse in comparing to Least Median Square..

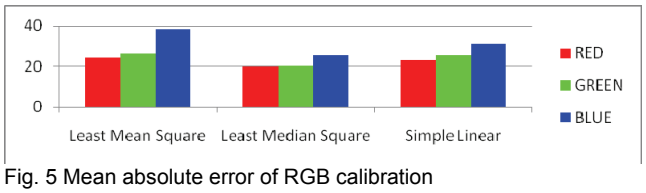

Fig. 5 Mean absolute error of RGB calibration

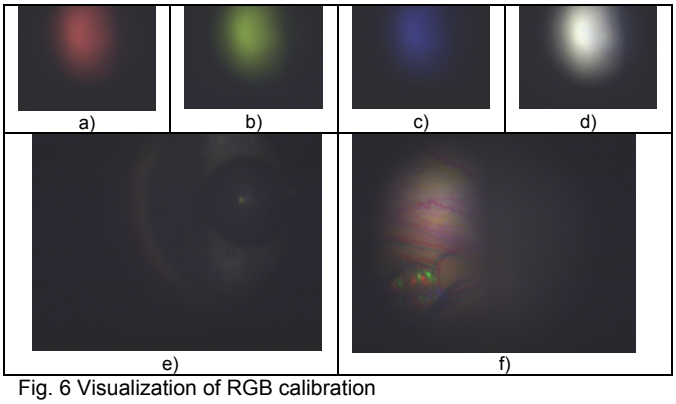

Fig. 6 Visualization of RGB calibration

In Fig. 6, the reconstruction results of original color images of the multispectral images represented colorchecker red, green, blue and white colors and two images of the front part of the eye are shown. The color

reconstruction is satisfactory – the colorchecker colors and eye structures colors are reconstructed properly. Probably explanation of the non zero absolute mean error is not uniform lighting of the colorchecker, which has not been taken into consideration in the train set preparation. The highest intensity is focused in the center area, noticeable weaker outside it.

The result of spectral space calibration are very similar. The mean absolute error is on the level of 5-10% of the global scale. There is no significant difference between approaches 1vs1 and ALLvs1. The greater noise for the short wavelengths results in their worse reconstruction, which can be noticed especially on the basis of relative absolute error analysis.

Determined calibration parameters are valid only for the same conditions – light source and acquisition parameters.

ACKNOLEDGMENT

This work was financed from the Polish Ministry of Science and Higher Education resources in 2009-2012 years as a research project.

REFERENCES

[1] Website of the PJWSTK Multispectral Group http://as.pjwstk.edu.pl , Accessed 1 August .2011

[2] Gat N.: Imaging spectroscopy using tunable filters: a review., Proc SPIE-Int SocOpt Eng. 2000

[3] Świtoński A., Michalak M., Josiński H., Wojciechowski K.: Detection of Tumor Tissue Based on the Multispectral Imaging, in Computer Vision and Graphics, Lecture Notes in Computer Science, Part 2, p. 325-333, Springer 2010.[4] Bieda R.,

[4] Bieda R., Świtoński A., , Kwiatek S., Latos W., Cieślar G., Sieroń AK lasyfikator jądrowej wersji maszyny wektorów podpierających wspomagający diagnostykę obszarów nowotworowych w wielospektralnym obrazowaniu endoskopowym, Przegląd Elektrotechniczny, (Electrical Review), 2010, R. 86 nr 12, s. 13-16,

[5] Zacher A., ŚwitońskiA., Bieda R., Kwiatek S., Latos W., Cieślar G., Sieroń A, Wojciechowski K.: Symulacyjne badania wybranych aspektów procesu endoskopowego obrazowania wielospektralnego, Przegląd Elektrotechniczny, (Electrical Review), 2010, 86(12), str. 170-174.

[6] Emiroglu M.,et al Is pseudoexfoliation syndrome associated with coronary artery disease?, North American Journal of Medical Sciences 2010, vol. 2, no 10

[7] Kurowska A.K, Kamińska A, Izdebska J, Szaflik JP, Szaflik J. *Zespół pseudoeksfoliacji (PEX) – schorzenie ogólnoustrojowe*. Klinika Oczna. 2009, 111 (4-6), 160-164.

[8] Stąpor K., Świtoński A.: Automatic analysis of fundus eye images using mathematical morphology and neural networks for supporting glaucoma diagnosis. Machine Vision and Graphics, 2004

[9] Tamura S., Okamoto Y.: Zero-crossing interval correction in tracing eye-fundus blood vessels. Pattern, Recognition, Vol. 21, No. 3, 227-233, 1988

[10] Pinz A., et al.: Mapping the human retina. IEEE Trans. Medical Imaging, Vol.1, 210-215. 1999

[11] Morris D.T., Donnison C.: Identifying the Neuroretinal Rim Boundary Using Dynamic Contours. Image and Vision Computing, Vol. 17, 169-174.

[12] Walter T., Klein J.: Segmentation of color fundus images of the human retina: detection of the optic disc and the vascular tree using morphological techniques. Proc. 2nd Int. Symp. Medical Data Analysis, 282-287, 2001

[13] Osareh A. et al.: Classification and Localisation of Diabetic-Related Eye Disease. 7th European Conference on Computer Vision (ECCV), Springer LNCS 2353, May, 502-516.2002

[14] Lowell J.: Optic nerve head segmentation. IEEE Trans. Medical Imaging, Vol.23, 256-264, 2004

[15] Staapor K, Pawlaczyk L., Chrastek R., Michelson G., Automatic Detection Of Glaucomatous Changes Using Adaptive Thresholding And Neural Networks, 2004

[16] Woolfe F., Maggioni M., Davis G., Warner F.,Coifman R., Zucker S.: Hyperspectral microscopic discrimination between normal and cancerous colon biopsies.,IEEE Transactions on Medical Imaging, VOL. 99, NO. 99, 1999

[17] Masood K., Rajpoot N Spatial Analysis for Colon Biopsy Classification from Hyperspectra in Annals of the BMVA Vol. 2008, No. 4, pp 1–16, 2008

[18] Rajpoot K., Rajpoot N. SVM Optimization for Hyperspectral Colon Tissue Cell Classification, in Medical Image Computing and Computer Assisted Intervention, 2004

[19] Carvalho, O.A., Carvalho, A.P.F. Guimaraes, R.F., Lopes, R.A.S., Guimaraes, Souza Martins, E. Pedreno, J.N., Classification of hyperspectral image using SCM methods for geobotanical analysis in the Brazilian savanna region, Geoscience and Remote Sensing Symposium, 2003. IGARSS '03. Proceedings. IEEE International, 2003

[20] P.H. Hsu, Feature extraction of hyperspectral images using matching pursuit, in ISPRS Journal of Photogrammetry and Remote Sensing Volume 62, Issue 2, p. 78-92 , 2007

[21] Lau D. Villis C., Furman S., Livett M.: Multispectral and hyperspectral image analysis of elemental and micro-Raman maps of cross-sections from a 16th century painting, in Analytica Chimica Acta Volume 610, Issue 1, p. 15-24, 2008

[22] Stąpor K., Świtonski A, Automatic detection of early sympthoms of diabetic retinopathy from fundus images using mathemathical morphology, Studia Informatica,…, 2004

[23] Stąpor K., Świtonski A, Blood vesssles segmentayion from fundus images using mathemathical morphology, Studia Informatica,…, 2004

[24] Sopharak A, Uyyanonvara B, Barman S., VongkittIrux S., Wongkamchang N, Fine Exudate Detection using Morphological Reconstruction Enhancement, International Journal of Applied Biomedical Engineering, vol. 1, no. 1, 2010

[25] *Walter T., Klein J., Massin P., Zana F.:* Automatic segmentation and registration of retinal fluorescein angiographies - Application to diabetic retinopathy First International Workshop on Computer Assisted Fundus Image Analysis (CAFIA) 2000

[26] Andor Luca Website, http://www.andor.com/scientific_cameras/luca, Accessed 1 August 2011

[27] Varispec Filters, http://www.spectralcameras.com/varispec Accessed 1 August 2011

[28] Witten I.H., Frank E.: Data Mining. Practical Machine Learning Tools and Techniques. 2nd edition, Elsevier, 2005

[29] Niżankowska M.H., *Jaskra.* Seria Basic and Clinical Science Cours, Urban & Partner, Wrocław 2006, 5-6

[30] Kanski J. et al. Glaucoma: a color manual of diagnosis and treatment. Butterworth-Heinemann

[31] Switonski A., Bieda R., Wojciechowski K, Multispectral imaging for supporting colonoscopy and gastroscopy diagnosis, monograph Human-Computer Systems Interaction. Backgrounds and Applications 2, Spriger-Verlag, 2011

[32] X-Rite Colorcheckers http://www.xrite.com, Accessed 1.8.2011

[33] Ocean Optics Spectrometers http://www.oceanoptics.com, Accessed 1.8.2011

***Authors**: dr inż. Adam Świtoński, Polsko-Japońska Wyższa Szkoła Technik Komputerowych, Aleja Legionów 2, 41-902 Bytom. E-mail aswitonski@pjwstk.edu.pl, prof. dr hab. inż. Tomasz Błachowicz, Politechnika Śląska, Instytut Fizyki, ul.Bolesława Krzywoustego 2, 44-100 Gliwice, E-mail: tomasz.blachowicz@polsl.pl, Marcin Zieliński, Katedra i Klinika Okulistyki Akademii Medycznej we Wrocławiu ,ul., .Borowska 213, E-mail: marcinosz@interia.pl, 50-530 Wrocław, prof. dr hab. Marta Misiuk Hojto Katedra i Klinika Okulistyki Akademii Medycznej we Wrocławiu ,ul. .Borowska 213, 50-530 Wrocław, E-mail: …, prof. dr hab. Inż. Konrad Wojciechowski, Polsko-Japońska Wyższa Szkoła Technik Komputerowych, Aleja Legionów 2, 41-902 Bytom. E-mail kwociechowski@pjwstk.edu.pl*